

# Enhance iris segmentation method for person recognition based on image processing techniques

Israa A. Hassan<sup>1</sup>, Suhad A. Ali<sup>1</sup>, Hadab Khalid Obayes<sup>2</sup>

<sup>1</sup>Department of Computer Science, College of Science for Women, University of Babylon, Babylon, Iraq

<sup>2</sup>Department of Geography, College of Education for Humanities Studies, University of Babylon, Babylon, Iraq

---

## Article Info

### Article history:

Received Mar 12, 2022

Revised Sep 27, 2022

Accepted Oct 26, 2022

---

### Keywords:

Biometrics

Canny edge detection

Hough transform

Iris recognition

Iris segmentation

---

## ABSTRACT

The limitation of traditional iris recognition systems to process iris images captured in unconstrained environments is a breakthrough. Automatic iris recognition has to face unpredictable variations of iris images in real-world applications. For example, the most challenging problems are related to the severe noise effects that are inherent to these unconstrained iris recognition systems, varying illumination, obstruction of the upper or lower eyelids, the eyelash overlap with the iris region, specular highlights on pupils which come from a spot of light during captured the image, and decentralization of iris image which caused by the person's gaze. Iris segmentation is one of the most important processes in iris recognition. Due to the different types of noise in the eye image, the segmentation result may be erroneous. To solve this problem, this paper develops an efficient iris segmentation algorithm using image processing techniques. Firstly, the outer boundary segmentation of the iris problem is solved. Then the pupil boundary is detected. Testes are done on the Chinese Academy of Sciences' Institute of Automation (CASIA) database. Experimental results indicate that the proposed algorithm is efficient and effective in terms of iris segmentation and reduction of time processing. The accuracy results for both datasets (CASIA-V1 and V4) are 100% and 99.16 respectively.

*This is an open access article under the [CC BY-SA](https://creativecommons.org/licenses/by-sa/4.0/) license.*



---

### Corresponding Author:

Suhad A. Ali

Department of Computer Science, College of Science for Women, University of Babylon

Babylon, Iraq

Email: suhad\_ali2003@yahoo.com

---

## 1. INTRODUCTION

Biometrics is the most promising system for identifying a user, where it is associated with uniquely human characteristics. Biometric authentication can be preferred over many traditional methods, such as smart cards and passwords because biometrics makes information difficult to steal [1]. Physiological traits such as fingerprints, DNA, facial recognition, iris, and so on, and behavioral characteristics such as voice, gait, signature, and so on, are the most frequent biometric identifiers [2].

Iris recognition is considered one of the important methods of ineffective personal identification. It has many applications in security systems, employee attendance, forensic investigations, and others. This is due to the complex pattern and uniqueness of the iris for each human being. Unlike other biometric methods such as fingerprints and faces, iris features don't change over time and have a low error rate in recognition. One of the most important steps in iris recognition is iris segmentation [3]. Usually, the input images of the eyes are in un-constrained conditions. Meaning the algorithm should detect and identify the iris area. This operation is considered complicated due to the noise and variation of the iris location [4]. Thus, iris location should be identified and detected first in order to process it later. Iris is an area characterized by its almost circular

shape between the pupil and the sclera and consists of a set of characteristics such as freckles, ridges, stripes, crypts, rings, ligaments, and zigzag patterns. These characteristics are unique, statistically stable, and dispersed randomly throughout the human iris. The iris is a secure and trustworthy source of personal identification because of these qualities [5]. Iris segmentation is the process of detecting the location of the iris area in the eye image. So, it will be used later to identify the identity of the person with that eye. It involves defining the inner and outer borders of the iris, which is crucial for the accuracy of iris recognition systems [6]. Additionally, this stage of segmentation also allows for the normalization of the iris region and the extraction of discriminative features from well-aligned iris samples [7].

The most effective and modern approaches in detecting the iris could be grouped into two general approaches [8]. The first approach involves using deep learning techniques. The second approach involves using two typical algorithms were proposed by Daugman (integro-differential operators) and Wildes (Hough transform) [9]. The methods for iris segmentation based on deep learning include the following: in 2018, Lozej *et al.* [10] proposed a model based on U-Net to perform iris segmentation. The architecture of U-Net is known in the medical image processing field due to its high performance on a relatively small dataset. It uses the encoder-decoder design. The encoder is performing classical convolutional neural networks (CNN) operations. In this work, the visual geometry group (VGG) model is used for the encoder. The decoder up-samples the lower layer's feature maps while also concatenating and cropping the encoder part's output of the same depth. The training technique employs adaptive moment estimate (Adam) and binary cross-entropy. Chinese Academy of Sciences' Institute of Automation (CASIA) database is used, with 160 images for the training phase, and 40 images for the testing phase. Accuracy ranged between 96% to 97% based on network depth and batch normalization [10]. Another U-Net based work is proposed in 2019 by Zhang *et al.* [11]. However, they extracted more global features using dilated convolution rather than original convolution to better process the details of images. In dilated convolution (FD-UNet), the convolutional mask has zero values inside of it (i.e., avoid some parts of the original image). This will lead to more receptive field information without increasing the complexity of the algorithm and losing the information. This method was tested on several databases, including CASIA, and the accuracy rate was 97.36% [11]. In 2019, Li *et al.* [12] presented a method composed of learning and edge detection algorithms for iris segmentation. The bounding box is found by faster region-based convolutional neural networks (R-CNN) that is built of six layers; the region of the pupil is detected by using a Gaussian mixture model. On the CASIA-Iris-Thousand database, experimental findings for this proposed technique obtained 95.49 % accuracy.

The methods for iris segmentation based on Daugman (integro-differential operators) and Wildes (Hough transform) include the following: Kennedy and others proposed a method for iris segmentation. It entails switching from the integro-differential operator approach (John Daugman's model) to the Hough transform (Wilde's model) as the segmentation strategy for this implementation. This study analyzed the two segmentation approaches in-depth to determine which is superior for recognition based on wavelet packet decomposition. The integro-differential technique to segmentation was found to be 91.39 percent accurate, whereas the Hough transform approach was found to be 93.06 percent accurate [13]. In 2020 Fathee *et al.* [14] proposed a new segmentation algorithm to segment iris images that captured in visible wavelength environments. This algorithm starts with the area of the iris that is easiest to recognize, the black, circular area known as the pupil, and reduces the deterioration and noise from there. Then, a circular Hough transform is used to precisely locate the iris. Finally, using a set of more appropriate techniques for unrestricted situations, the upper and lower eyelids and eyelashes are identified and eliminated from the iris region. The efficacy and stability of the proposed method are confirmed by comparison with a number of cutting-edge segmentation algorithms. Sahnoud and Fathee [15] in 2020 and by taking into account the color information from various color spaces, a unique and quick segmentation technique to handle eye images acquired in visible wavelength surroundings has been suggested. An acceptable collection of color models is chosen for the segmentation process after an analysis of the numerous available color spaces, including red, green, blue (RGB), YCbCr, and hue, saturation, value (HSV). A number of practical strategies are used to identify and eliminate non-iris regions such the pupil, specular reflection, eyelids, and other in order to precisely pinpoint the iris region. Experimental results prove the efficiency of this method in terms of accuracy and implementation time. In 2021, Tahir *et al.* [5] proposed a method for iris segmentation. In this method for pupil boundary detection, processes such as morphological filtering and two-direction scanning were applied. The Wildes approach is adjusted for limbic border identification by limiting the Canny edge detector and Hough transform processes to a tiny region of interest (ROI) not exceeding 20% of the picture area. This method was tested on several databases, including CASIA-V1 and V4, and the accuracy rate was 96.48 to 95.1 respectively. In 2022, Khan *et al.* [16] presented a compound method to perform the iris segmentation based on several techniques such as Laplacian of Gaussian (LoG) filter, region growing (one of the ways to segment images), and zero-crossings of the LoG filter. In this suggested method, to detect the pupil region used LoG filter with region growing, and used zero-crossings of the LoG filter to correctly identify the boundaries of the inner and outer circular iris. This method has been tested on several public

databases including CASIA-V1 and CASIA-V3. The segmentation accuracy of the proposed method was good and outperformed many methods.

There are many problems and obstacles that can face the process of extracting the iris from the image of the eye such as the background may be isolated and may be complex something, noise removal, enhance image contrast, rotate in different directions, obstruction of the upper or lower eyelids, the eyelash overlaps with iris region, specular highlights on pupil which come from spot of light, and decentralization of iris image which caused by the person's gaze. This paper aims at introducing an enhanced method for iris localization robust against these problems. This paper is structured as: section 2 introduces the layout of the proposed iris segmentation system. Section 3 describes the results and discussion of conduct tests. Finally, the derived conclusions of this paper are shown in section 4.

## 2. METHOD

In this work, the goal is to detect the required area of the eye which is the iris area, without the pupil area. Since the images in the dataset are for eye images, we noticed that there is a common feature that could be based on detecting the iris region. Each image has a central and almost cycle in the middle of the image, with a darker color than the area around it which represents the pupil area. The capacity of the image processing system to properly locate and distinguish the iris pattern in the input eye image is a key stage of the biometric recognition process. An automatic algorithm of segmentation was utilized, which would localize the iris region from an eye image by applying two stages. The first stage, detection outer iris boundary, and the second stage detection the inner iris boundary (pupil boundary) as shown in Figure 1 until we finally determine the ROI, which is the iris of the eye only, as shown in Figure 2.

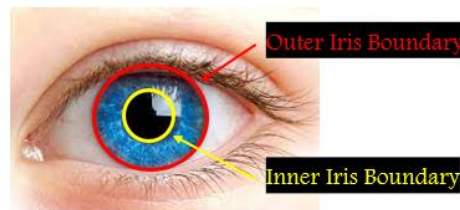


Figure 1. Explain outer and inner iris boundary

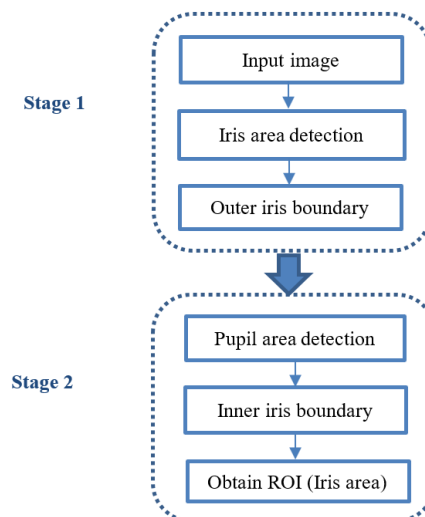


Figure 2. General diagram for iris detection

### 2.1. Stage 1: outer iris boundary detection

Segmentation of the outer boundary of the iris image was achieved through using the circular Hough transform (HT). This mechanism can determine these circular boundaries even if the circle is unclear or incomplete, and it also achieves high accuracy in the process of determination [17], [18]. In this stage, the iris is separated from the eye image using steps depicts in Figure 3.

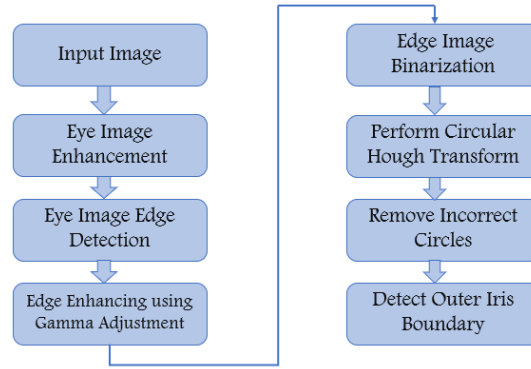


Figure 3. Outer iris boundary detection steps

### 2.1.1. Eye image enhancement

Two interface regions (pupil/iris) and (iris/sclera) make up the eye image. To make the iris border more visible, we will first use a contrast stretching-based mapping approach on the original eye image as shown in Figure 4(a), using (1).

$$E - Img(X, Y) = \begin{cases} 0 & I(x, y) \leq Low \\ 255 \times \frac{I(x, y) - Low}{High - Low} & \text{if } Low < I(x, y) < High \\ 255 & I(x, y) \geq High \end{cases} \quad (1)$$

Where low, high is the lowest and highest gray-levels in an image, respectively. As shown in Figure 4(b).

### 2.1.2. Eye image edge detection

To detect the iris of the eye, the first step will be to apply canny edge detection on the image. This will convert the image into lines that represent the edge of the image. Canny edge detection is the process of finding the intensity gradient of the image first [1]. Then a threshold value is applied to suppress the small and irrelevant parts of the image, for this edge map, the hysteresis threshold will be applied. With this operation, the values of the image above and below a threshold value will be omitted. The result of this step is shown in Figure 4(c). The goal of this step is to ensure that the important edges are kept together, with no multiple edge parts [19].

### 2.1.3. Edge enhancing using gamma adjustment

The edges obtain from the previous step are not very clear therefore gamma adjustment with ( $\gamma = 1.9$ ). Is applied to enhance the contrast of images according to (2).

$$G\_Img(i, j) = c \times E\_Img(i, j)^\gamma \quad (2)$$

The result of this edge enhancement step is shown in Figure 4(d).

### 2.1.4. Edge image binarization

In this step, the gamma enhanced image is converted to a binary edge image. Hysteresis thresholding method is used which needs two threshold T1, and T2. All pixels with value greater than T1 are considered edges. All pixels with values over threshold T2 that are next to points that have been defined as edges are also marked as edges. Eight connectivity is utilized, as shown in Figure 4(e).

### 2.1.5. Iris boundary detection (perform circular Hough transform)

In the edge image, there are more circular edges along the iris boundary, and a circular Hough transform will be used. In Hough transform, the goal is to find the features that match the predefined shape. Since in Hough transform, only regular and predefined shapes could be detected, such as lines and circles. Even if the circles are not clear and incomplete, Hough transform could identify them. Since the equation of the circle is containing three variables ( $a$ ,  $b$ , and  $r$ ) as shown in (3). Where  $r$ , is the circle radius.  $a$  and  $b$  are the cycle values on the two axes [20].

$$(x_i - a)^2 + (y_i - b)^2 = r^2 \quad (3)$$

Circular Hough transform works by taking each point in the original image, and rendering it on the space of the values of  $a$  and  $b$ . This will result in creating a cycle in the Hough space for each point in the original image. If the created cycles in the Hough images are intersected in a single point, and by following the voting concept (i.e. more points meaning stronger evidence to indicate there is a circle), the point of which there are many cycles are intersected on indicating there is a cycle in the original image [21]. Figure 4(f) shows how the proposed method steps on detecting the outer Iris boundary by using circular Hough transform.

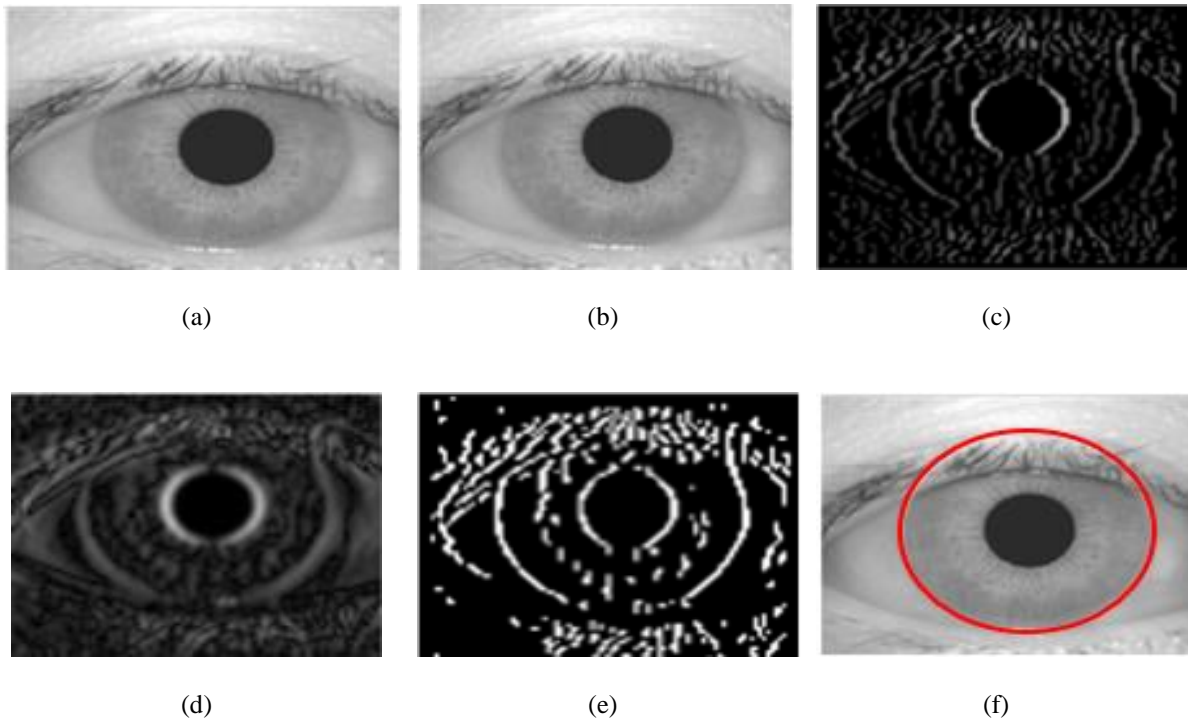


Figure 4. Resultant images of iris boundary: (a) original image, (b) enhanced image, (c) image after canny edge detection, (d) image after gamma correction, (e) binarized edge image, and (f) resultant image with iris boundary

## 2.2. Stage2: inner iris boundary detection

The behavior of image intensity in both the pupil and iris of the sections of the eye is taken into account to detect the inner circle of the iris which is the pupil area. The overall intensity value in the pupil area of the complete eye image is smaller than it is in other locations. Aside from that, the pupil is the largest linked and densely packed black area in the eye image. As a result, the processes in Figure 5 were used to obtain the benefits of these qualities.

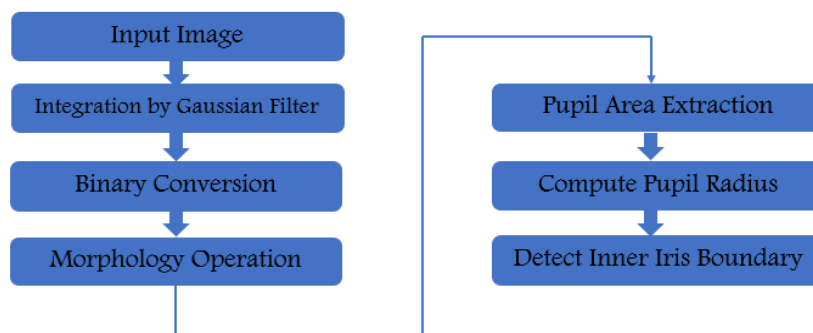


Figure 5. Pupil region detection

### 2.2.1. Integration by Gaussian filter

In the first step, to eliminate the effect of artifacts in the image of the eye as shown in Figure 6(a) which represents the eye image before smoothing. A smoothing for the entire eye image is applied by using a Gaussian filter with mask size (11×11). Gaussian filter is a linear smoothing filter that is suitable for eliminating noise, it's used to smooth the noises, by blurring the original image. In the Gaussian filter, the process is to apply the 2D kernel on the original image. The kernel coefficients of Gaussian decrease, when the distance from the center of the kernel increase. Moreover, the center values of the kernel hold more weight than the values on the edges of the kernel. The (4) represents the equation used to generate the Gaussian filter on the image.

$$G - Img(x, y) = \frac{1}{2\pi\sigma^2} e^{-\frac{x^2+y^2}{2\sigma^2}} \quad (4)$$

Where,  $\sigma$  is the standard deviation of the distribution. The larger the value of  $\sigma$ , the greater the blurring is [22]. The result of this step is shown in Figure 6(b).

### 2.2.2. Binary conversion

The correct intensity value to employ as a threshold to binarize the image into two types of pixels (pupil and non-pupil) should be found in this step. The challenge of determining an ideal threshold value suitable to all eye images can be regarded as unreasonable due to the broad range of brightness distribution differences of eye images. Furthermore, for every threshold value, some pixels may not belong to the pupil area and have an intensity value lower than the threshold value. To address these two issues, a threshold value is generated using first-order statistical analysis based on the intensity distribution, and steps of cleaning are used to the resulting binary image to eliminate non-pupil pixels. The image histogram is divided into five bins, since the pupil pixels have the lowest value near or equal to zero. The gray level  $G$  that corresponds to an average of histogram bins (1 and 2) will be used as a threshold as in (5).

$$G = (img_{Bin(1)} + img_{Bin(2)})/2 \quad (5)$$

Where,  $img_{Bin}(i)$  represents the histogram frequencies at gray level  $i$ .

In general, all intensity values below ( $T$ ) in the eye image are changed to 1 (consider as object), and all intensity values above or equal to  $T$  are changed to 0 (consider as background), that is:

$$Bim(x, y) = \begin{cases} 1 & \text{if } I(x, y) \leq T \\ 0 & \text{otherwise} \end{cases} \quad (6)$$

Where  $I(x, y)$  represent the intensity value at location  $(x, y)$ , and  $Bim(x, y)$  is the pixel value that has been converted. The result of this step is in Figure 6(c).

### 2.2.3. Morphology operation

Eye image contains in the pupil region white points. In CASIA-V4, the pupil region contains eight roughly white dots randomly located inside it. The main white segment is represented by the backdrop area (i.e., the area surrounding the pupil region), and the other white spots are reflection locations inside the pupil (which should convert to black points). To detect the presence of these reflection points, the closing morphology process with the kernel (11×11) is used to the resulting (pupil/non-pupil) binary images [23] as shown in Figure 6(d).

### 3.2.4. Pupil area extraction

To collect the pupil region the connected components in a 2-D binary image are extracted by using 8-neighbors. Then the area of each connected compothe nent is computed according to:

$$A_i = \sum_{x=0}^{M-1} \sum_{y=0}^{N-1} bim(x, y) \quad (7)$$

Then the component with the largest area represents the pupil region [24]. The pupil center  $(X_p, Y_p)$  is calculated by averaging the coordinates of the points in the pupil region using:

$$x_p = \frac{1}{N} \sum_{i=1}^N x_i, \quad y_p = \frac{1}{N} \sum_{i=1}^N y_i \quad (8)$$

Where,  $N$  is the number of collected points in pupil regions. The reslts for this stage shown in Figure 6(e).

### 2.2.5 Compute pupil radius

To find pupil radius we move around the four directions (top, right, down, and left) from the specified point  $(xp, yp)$ . For each direction, we find the first background pixel. Let  $x_l$  be the first background pixel detected on the left side of the line  $(y = yp)$  during the horizontal scan, and  $x_r$  be the first background pixel found on the right side of the same horizontal scan. The horizontal radius,  $R_h$ , is then calculated:

$$R_h = \frac{1}{2}(x_l - x_r) \quad (9)$$

When a vertical scan is done down the column  $(x = xp)$ , let  $x_b$ ,  $x_t$  be the first met background pixels to the bottom and top sides, respectively.  $R_v$  is the vertically assessed radius, and it's calculated like this:

$$R_v = \frac{1}{2}(x_t - x_b) \quad (10)$$

Then, the pupil radius  $R_p$  can be calculated as:

$$R_p = \frac{1}{2}(R_h + R_v) \quad (11)$$

The results for this stage shown in Figure 6(f).

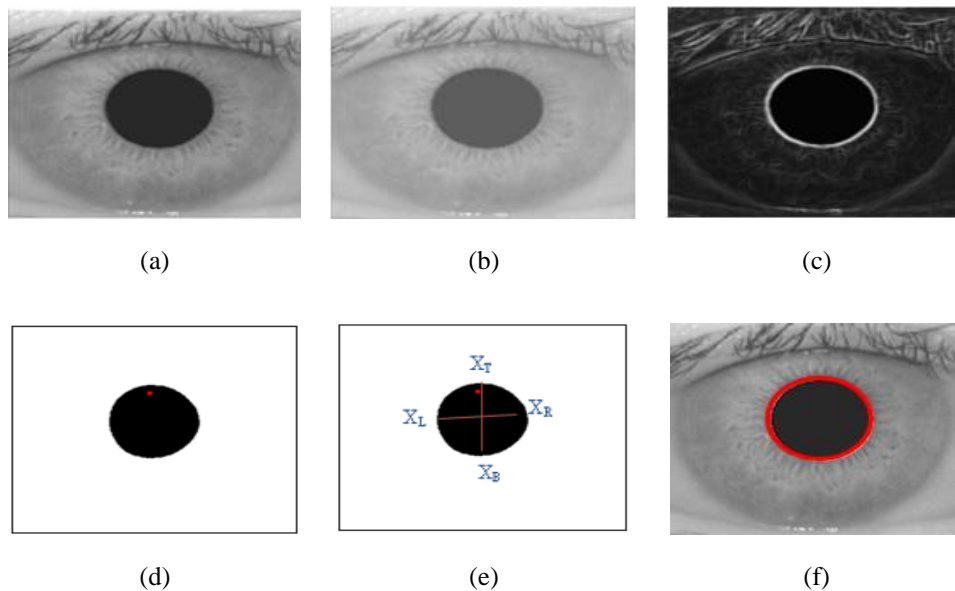


Figure 6. Results of pupil segmentation for CASIA-V1 dataset: (a) input image (original), (b) image after smoothing, (c) convert to a binary image, (d) applying the morphology operation and reflection point removal results, (e) the pupil region with four directions, and (f) detected pupil region

## 3. RESULTS AND DISCUSSION

To evaluate the performance of the proposed method, we use iris images obtained from CASIA-V1.0 and CASIA-V4.0 iris image datasets. The results will be evaluated by calculating the accuracy of the correctly detected iris in the dataset. The followed accuracy equation is written as in (12).

$$Accuracy = \frac{\text{number of correctly segmented images}}{\text{number of total images}} \times 100 \quad (12)$$

### 3.1. Iris image dataset

CASIA iris image dataset V1 was utilized as the dataset. The centre for biometrics and security research compiled this dataset. The CASIA iris image dataset, version 1.0, contains 756 images from 108 different persons. There are seven images for each eye[25]. Each iris image has a resolution of  $280 \times 320$  pixels and is in grayscale. There are 2639 iris images in CASIA version 4.0 (interval class). All iris images are 8-bit gray-level JPEG files that were captured or produced under near-infrared illumination. Each iris image is  $280 \times 320$  pixels and is grayscale (256 levels) [26].

### 3.2. Results of iris boundary segmentation

Iris boundary segmentation is achieved by determining the geometrical parameters of the iris, namely the iris center and radius (inner and outer). The suggested method's results on several randomly selected images from the CASIA-V1 (as shown in Figure 7(a)) and CASIA-V4 (as shown in Figure 7(b)) datasets. The results show the performance of the proposed method against different previously mentioned problems that can be arisen during iris segmentation process such as varying illumination, obstruction of the upper or lower eyelids, and the eyelash overlaps with iris region.

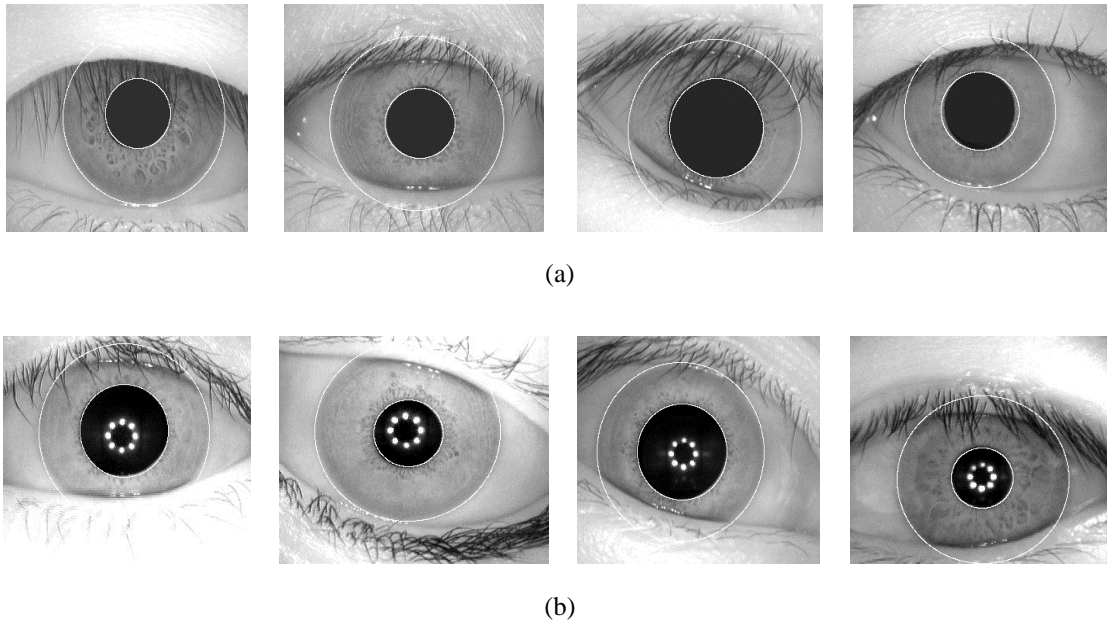


Figure 7. Samples of accurate iris Segmentation results for images belong to (a) CASIA1 dataset and (b) CASIA4 dataset

The accuracy is about (100%) for CASIA-V1 for both inner and outer boundaries. For CASIA-V4 the accuracy is about (99.60) for the inner boundary and (99.16) for the outer boundary. To evaluate the performance of the new method, and show that its results are better than those of the existing experiments. This section reviews the results of our proposed method and comparison with many previously published studies that use the CASIA iris datasets. Table 1 shows the comparison of the overall accuracy with several existing methods for CASIA-Iris Dataset with its many versions.

Table 1. Comparison our method with some recent segmentation methods on CASIA dataset

Method in reference	A version of CASIA-iris dataset	Overall accuracy
U-Net [6]	CASIA-V1	Ranging (96% – 97%)
FD-UNet [7]	CASIA-V4	97.36%
Faster R-CNN [8]	CASIA-V4	95.49%
Seg. by circular HT [9]	CASIA-Iris	Integro-differential (91.39%) Circular HT (93.06%)
Iris localization (image processing techniques) [10]	CASIA-V1, CASIA-V4	96.48% – 95.1%
Proposed method	CASIA-V1, CASIA-V4	100% – 99.16%

## 4. CONCLUSION

Segmentation is an important part of the iris recognition system. Since it is important to detect the iris area first before any further process could be conducted. In this work, the iris segmentation method is developed. This method consists of two stages, first: detects the outer iris boundary by applying a number of steps: eye image enhancement, edge detection by using a Canny edge detector, gamma adjustment, image binarization and applying circular Hough transform. Second: detect the inner iris boundary by applying: Gaussian filter, binarized image by histogram thresholding, morphology operation and compute pupil radius to detect pupil boundary that represents inner iris boundary. Combining gamma transform and histogram enhancement techniques is particularly useful for separating eyelash and eyelid traces that may occur in the iris region.

The inclusion of some first-order statistical factors is critical for pupil localization since iris images are sensitive to variable illumination, making the use of a fixed threshold value unfeasible. The pupil region is determined in the proposed technique by employing an adaptive threshold, whose value is obtained from the intensity distribution and first-order statistical analysis. The method is tested on CASIA iris image dataset V1 and V4. The accuracy results for both datasets are 100% and 99.16 respectively. The future work will involve using these segmented iris images to develop a sophisticated iris recognition system.

## ACKNOWLEDGEMENTS

This work was supported by Department of Computer Science, College of Science for Women, Babylon University, Babylon, Iraq.

## REFERENCES

- [1] K. Kumar K., R. Bharadwaj M., Shesank Ch, and Sujana S., "Effective Deep Learning approach based on VGG-Mini Architecture for Iris Recognition," *Annals of the Romanian Society for Cell Biology*, vol. 25, no. 5. pp. 4718–4726, 2021. [Online]. Available: <https://www.annalsofscb.ro/index.php/journal/article/view/5760/4476>
- [2] J. J. Winston and D. J. Hemanth, "A comprehensive review on iris image-based biometric system," *Soft Computing*, vol. 23, pp. 9361–9384, 2019, doi: 10.1007/s00500-018-3497-y.
- [3] P. Podder, A. H. M. Parvez, M. M. Rahman, and T. Z. Khan, "Ramifications and Diminution of Image Noise in Iris Recognition System," in *Proc. of 2018 IEEE International Conference on Current Trends toward Converging Technologies*, 2018. [Online]. Available: <https://arxiv.org/ftp/arxiv/papers/2002/2002.03125.pdf>
- [4] M. S. Nixon and A. S. Aguado, *Feature Extraction and Image Processing for Computer Vision*, London, United Kingdom: Academic press, 2019. [Online]. Available: <https://www.sciencedirect.com/book/9780123965493/feature-extraction-and-image-processing-for-computer-vision>
- [5] A. A. K. Tahir, S. S. Dawood, and S. Anghelus, "An Iris Recognition System Using A New Method of Iris Localization," *International Journal of Open Information Technologies*, vol. 9, no. 7, 2021. [Online]. Available: <http://injoit.org/index.php/j1/article/view/1111/1094>
- [6] J. Oyeniyi, O. Oyeniran, L. Omotosho, and O. Adebayo, "Iris Recognition System: Literature Survey and Technical Overview," *International Journal of Engineering and Artificial Intelligence*, vol. 1, no. 3, pp. 34–43, 2020. [Online]. Available: [https://d1wqtxts1xzle7.cloudfront.net/65408591/5JIEAITECAP3-libre.pdf?1610487574=&response-content-disposition=inline%3B+filename%3DIris\\_Recognition\\_System\\_Literature\\_Surve.pdf&Expires=1672368702&Signature=A6CrJ0mfIPTnCMeE9aehfrsbaLxaLyTor6JaoH5t9C6hEC5qEH9vXaTCczjxL9EgYw34qLD2we7QJO0TjJysdOR0iK0xFOkBF7BjtGTzUBNzEWdkspkYHio1ZU3cGZL-dnaX2gxPrn2P3GwKwG09DjkaqT8FDomwH-8HQGQPGW-vN9SxxBv9RDnN0~o6y1tb~yggxReuImrlgTo9jtEzx2j~mDvnMI4fFSiGbkFww2MJpMELv5UfP~ItEHXDNfjMDoUY8UxMX8GuavkrJjpQBjCvQmKFFWp1wMBzou-zKOABASXypjWeso9RJW5ZeAJiyy4nkSyjcPjKZOy~l2QA\\_&Key-Pair-Id=APKAJLOHF5GGSLRBV4ZA](https://d1wqtxts1xzle7.cloudfront.net/65408591/5JIEAITECAP3-libre.pdf?1610487574=&response-content-disposition=inline%3B+filename%3DIris_Recognition_System_Literature_Surve.pdf&Expires=1672368702&Signature=A6CrJ0mfIPTnCMeE9aehfrsbaLxaLyTor6JaoH5t9C6hEC5qEH9vXaTCczjxL9EgYw34qLD2we7QJO0TjJysdOR0iK0xFOkBF7BjtGTzUBNzEWdkspkYHio1ZU3cGZL-dnaX2gxPrn2P3GwKwG09DjkaqT8FDomwH-8HQGQPGW-vN9SxxBv9RDnN0~o6y1tb~yggxReuImrlgTo9jtEzx2j~mDvnMI4fFSiGbkFww2MJpMELv5UfP~ItEHXDNfjMDoUY8UxMX8GuavkrJjpQBjCvQmKFFWp1wMBzou-zKOABASXypjWeso9RJW5ZeAJiyy4nkSyjcPjKZOy~l2QA_&Key-Pair-Id=APKAJLOHF5GGSLRBV4ZA)
- [7] A. Uhl, C. Busch, S. Marcel, and R. Veldhuis. (2020). *Handbook of Vascular Biometrics*. [Online]. Available: <https://link.springer.com/book/10.1007/978-3-030-27731-4>
- [8] H. J. Abdelwahed, A. T. Hashim, and A. M. Hasan, "Segmentation Approach for a Noisy Iris Images Based on Hybrid Techniques," *Engineering and Technology Journal*, vol. 38, no. 11, pp. 1684–1691, 2020, doi: 10.30684/etj.v38i11A.450.
- [9] Y. Y. Wei, A. Zeng, X. Zhang, and H. Huang, "Improvement of iris location accuracy in iris recognition," in *Proc. SPIE 12065, AOPC 2021: Optical Sensing and Imaging Technology*, 2021, doi: 10.1117/12.2607061.
- [10] J. Lozej, B. Meden, V. Struc, and P. Peer, "End-to-End Iris Segmentation Using U-Net," in *2018 IEEE International Work Conference on Bioinspired Intelligence (IWOB)*, 2018, pp. 1–6, doi: 10.1109/IWOB.2018.8464213.
- [11] W. Zhang, X. Lu, Y. Gu, Y. Liu, X. Meng, and J. Li, "A Robust Iris Segmentation Scheme Based on Improved U-Net," *IEEE Access*, vol. 7, pp. 85082–85089, 2019, doi: 10.1109/ACCESS.2019.2924464.
- [12] Y. -H. Li, P. -J. Huang, and Y. Juan, "An Efficient and Robust Iris Segmentation Algorithm Using Deep Learning," *Mobile Information Systems*, 2019, doi: 10.1155/2019/4568929.
- [13] K. Okokpujie, E. N. -Osaghae, S. John, and A. Ajulibe, "An improved iris segmentation technique using circular hough transform," *IT Convergence and Security 2017: Lecture Notes in Electrical Engineering*, vol. 450. pp. 203–211, 2017, doi: 10.1007/978-981-10-6454-8\_26.
- [14] H. N. Fathee, S. Sahmoud, and J. M. A. -Jabbar, "A Robust Iris Segmentation Algorithm Based on Pupil Region for Visible Wavelength Environments," in *2020 3rd International Seminar on Research of Information Technology and Intelligent Systems (ISRITI)*, 2020, pp. 655–660, doi: 10.1109/ISRITI51436.2020.9315343.
- [15] S. Sahmoud and H. N. Fathee, "Fast Iris Segmentation Algorithm for Visible Wavelength Images Based on Multi-color Space," in *International Conference on Advanced Concepts for Intelligent Vision Systems (ACIVS 2020)*, 2020, pp. 239–250, doi: 10.1007/978-3-030-40605-9\_21.
- [16] T. M. Khan, D. G. Bailey, and Y. Kong, "A fast and accurate iris segmentation method using an LoG filter and its zero-crossings," *arXiv preprint*, 2022. [Online]. Available: <https://arxiv.org/pdf/2201.06176.pdf>
- [17] P. Mukhopadhyay and B. B. Chaudhuri, "A survey of Hough Transform," *Pattern Recognition*, vol. 48, no. 3, pp. 993–1010, 2015, doi: 10.1016/j.patcog.2014.08.027.
- [18] M. Arsalan *et al.*, "Deep learning-based iris segmentation for iris recognition in visible light environment," *Symmetry*, vol. 9, no. 11, 2017, doi: 10.3390/sym9110263.
- [19] M. Kalbasi and H. Nikmehr, "Noise-Robust, Reconfigurable Canny Edge Detection and its Hardware Realization," *IEEE Access*, vol. 8, pp. 39934–39945, 2020, doi: 10.1109/ACCESS.2020.2976860.
- [20] N. Cherabit, F. Z. Chelali, and A. Djeradi, "Circular Hough Transform for Iris localization," *Science and Technology*, vol. 2, no. 5, pp. 114–121, 2012, doi: 10.5923/j.scit.20120205.02.
- [21] I. A. Qasmieh, H. Alquran, and A. M. Alqudah, "Occluded iris classification and segmentation using self-customized artificial intelligence models and iterative randomized Hough transform," *International Journal of Electrical and Computer Engineering (IJECE)*, vol. 11, no. 5, pp. 4037–4049, 2021, doi: 10.11591/ijece.v11i5.pp4037-4049.

- [22] M. P. Deisenroth, R. D. Turner, M. F. Huber, U. D. Hanebeck, and C. E. Rasmussen, "Robust Filtering and Smoothing with Gaussian Processes," *IEEE Transactions on Automatic Control*, vol. 57, no. 7, pp. 1865–1871, 2012, doi: 10.1109/TAC.2011.2179426.
- [23] F. F. -Hurtado, V. Naranjo, J. A. D. -Mas, and M. Alcañiz, "A hybrid method for accurate iris segmentation on at-a-distance visible-wavelength images," *EURASIP Journal on Image and Video Processing*, 2019, doi: 10.1186/s13640-019-0473-0.
- [24] P. Zheng, D. Qin, B. Han, L. Ma, and T. M. Berhane, "Research on feature extraction method of indoor visual positioning image based on area division of foreground and background," *ISPRS International Journal of Geo-Information*, vol. 10, no. 6, 2021, doi: 10.3390/ijgi10060402.
- [25] Y. Wu *et al.*, "Enhanced Classification Models for Iris Dataset," *Procedia Computer Science*, vol. 162, pp. 946–954, 2019, doi: 10.1016/j.procs.2019.12.072.
- [26] L. Omelina, J. Goga, J. Pavlovicova, M. Oravec, and B. Jansen, "A survey of iris datasets," *Image and Vision Computing*, vol. 108, 2021, doi: 10.1016/j.imavis.2021.104109.

## BIOGRAPHIES OF AUTHORS



**Israa A. Hassan**    Currently, Israa is a Master student in Computer Science Department, Science College, and University of Babylon, Iraq. She received the B.Sc. degree in computer science on 2008 from Department of Computer Science, Babylon University. Her research interests include image processing, deep learning, pattern recognition. She can be contacted at email: Israa.kazem.gsci2@student.uobabylon.edu.iq.



**Suhad A. Ali**    She is working as Professor in Computer Science Department, Science College for Women, University of Babylon, Iraq. She received M.S. and Ph.D. degrees from Department of Computer Science, Babylon University in 2002 and 2014, respectively. Her areas of interest are digital image and video processing, pattern recognition and information hiding. She can be contacted at email: suhad\_ali2003@yahoo.com, wsci.suhad.ahmed@uobabylon.edu.iq.



**Hadab Khalid Obayes**    is assistant professor at University of Babylon, Babel, Iraq. She received her PhD degree from University of Babylon, Iraq, in 2020. She published a number of papers in scopus and international journals and referred conferences. Her current research areas are, AI, Machine learning, neural networks, deep learning, natural language processing and Image Processing. Email: hedhabsa@gmail.com, hedhab@uobabylon.edu.iq.